THE IRON AND OXYGEN ABUNDANCES IN THE METAL-POOR STAR HD 140283 AND IN THE SUN

N. G. Shchukina[1], **I. E. Vasiljeva**[1], **J. Trujillo Bueno**[2]

[1] *Main Astronomical Observatory, NAS of Ukraine*
27 Akademika Zabolotnoho Str., 03680 Kyiv, Ukraine
e-mail: shchukin@mao.kiev.ua

[2] *Instituto de Astrofísica de Canarias*
38205 La Laguna, Tenerife, Spain

We present the results of a theoretical investigation of the impact of NLTE effects and of granulation inhomogeneities on the iron and oxygen abundances in the metal-poor star HD 140283 and in the Sun. Our analysis is based on both the classical one-dimensional (1D) stellar atmosphere models and on a new generation of three-dimensional (3D) hydrodynamical models. We consider the Sun as a reference star. The solar iron and oxygen abundances are redefined.

INTRODUCTION

An accurate determination of the oxygen and iron abundance in late type stars has fundamental importance for constraining models of the chemical evolution of the Galaxy, for estimating the yields of light elements due to spallation processes in the interstellar or circumstellar gas, for testing different scenarios of nucleosynthesis in supernovae, *etc.* Such studies largely rely upon semi-empirical relations between elemental abundance ratios $[\mathrm{O/Fe}] = \log(\mathrm{O/Fe})_{\mathrm{star}} - \log(\mathrm{O/Fe})_{\odot}$ versus the stellar metallicity ([Fe/H] (*e.g.*, [4, 19, 25, 27, 34], and references therein).

There is a strong debate on the shape and spread of the [O/Fe] − [Fe/H] relation. First of all, the controversy discussed is linked with discordant results obtained using different indicators of the oxygen abundance, such as: i) the oxygen [O I] forbidden $\lambda\,6300$ Å line; ii) the oxygen O I infrared triplet at 7772–5 Å; iii) the molecular OH lines in the near ultraviolet; iv) the OH lines in the infrared. More precisely, the oxygen abundance derived using all of these indicators agrees with each other for moderate metal-deficient disc stars having $-1 \leq [\mathrm{Fe/H}] \leq 0$. However, there are clear discrepancies among the results obtained for metal-poor halo stars with metallicities $[\mathrm{Fe/H}] < -1$. The [O/Fe] ratio obtained appears to be independent of the stellar metallicity with a plateau between +0.4 and +0.5 dex in the metallicity range $-3 < [\mathrm{Fe/H}] < -1$ (see [5, 10, 13, 17, 24, 25]) or to increase linearly with decreasing metallicity ([1, 11, 14, 18, 19, 26, 36] and references therein) reaching $[\mathrm{O/Fe}] \simeq +1$ dex at $[\mathrm{Fe/H}] = -3$. On the other hand, Nissen *et al.* [27] concluded that there is a quasi-linear trend below $[\mathrm{Fe/H}] < -2$ with $[\mathrm{O/Fe}] \simeq +0.5$ dex at $[\mathrm{Fe/H}] = -2.5$ while estimates made by Asplund [4] point to a nearly flat [O/Fe] trend, but with a slow rise for $[\mathrm{Fe/H}] \leq -2$ between a plateau at $\simeq +0.4$ dex and Nissen's *et al.* [27] quasi-linear slope.

The another problem related with the [O/Fe] − [Fe/H] relation in metal-poor stars is the reliability of the iron abundance determinations. It is well known that the Fe I lines suffer from UV overionization in the atmospheres of late-type stars [9, 28, 31]. This NLTE effect tends to be substantially more important in metal-poor stars than in solar-like stars as a result of the lower electron density and of the weaker UV blanketing [19, 20, 30, 31, 35].

It is of interest to point out that while the Fe I lines are expected to be sensitive to the UV overionization mechanism, the LTE approximation is thought to be suitable for weak lines of Fe II (see, *e.g.*, [8, 27]). However, this does not have to be necessarily the case because many subordinate Fe II lines whose upper levels are of odd parity (starting at $z^6\mathrm{D}^{\mathrm{o}}$) might be partially filled by emission due to an optical pumping mechanism similar to that investigated by Cram *et al.* [15] for the solar case.

The solar photospheric oxygen and iron abundances used as as a reference for stellar metallicity determinations are also under discussion (see [3, 23, 29, 31]).

Possible reasons for the oxygen and iron abundance discrepancies in metal-poor stars are widely discussed in the literature (*e.g.*, [21, 26, 34, 35], and references therein). All abundance indicators in metal-poor stars are to a different degree sensitive to the adopted stellar parameters (T_{eff}, $\log g$, and [Fe/H]). They also have to depend on the atmospheric structure properties such as the temperature gradient and the ratio of the line to continuous opacity. Large uncertainties could result from neglecting granulation produced by the stellar surface convection which dominates in late type stars. Part of the discrepancies are probably due to NLTE effects. Errors in the measurements of equivalent widths are of minor importance with the exception of weak [O I] and Fe II lines [19].

The recent generation of three-dimensional (3D) hydrodynamical models of stellar atmospheres have activated the present debates on the influence of granulation inhomogeneities and of NLTE effects on the determination of chemical abundances in metal-poor stars (see [4–6, 8, 27, 30, 31]). These debates make evident that detailed, 3D+NLTE investigations of the iron and oxygen abundances in the photospheres of metal poor stars and the Sun are urgently needed. It is crucial that this type of analyses has to be carried out *jointly* for iron and oxygen, using the same atmospheric and atomic models, atomic line parameters and radiative transfer codes.

This paper presents the results of such an investigation. We study the NLTE formation problem of the Fe I, Fe II, and O I lines in a three-dimensional hydrodynamical model of the atmosphere of the metal-poor star HD 140283. This classical halo subgiant is widely used for studies of a very early Galaxy and the origin of the chemical elements. In order to quantify the impact of 3D simulations on the abundance determinations in HD 140283 we carry out a detailed comparison with the 1D classical modelling. To this end, we use Asplund's *et al.* 3D hydrodynamical model [8] of the star HD 140283, as well as a suitable grid of Kurucz's 1D models. Moreover, we evaluate the extent to which 3D+NLTE effects influence the determination of the stellar parameters of this metal-poor subgiant.

Our paper also considers the case of the Sun as a reference for stellar abundance determinations with emphasis on the solar oxygen abundance derived from the O I IR triplet. As in our NLTE+3D analysis of the solar iron abundance [31] here we investigate the solar oxygen abundance problem by using the same 3D hydrodynamical solar granulation model [7, 33]. For a more detailed presentation and discussion of the implications of our results see [32].

THE METHOD, OBSERVATIONS AND ATOMIC MODELS

We applied an efficient multilevel transfer code that we have developed thinking in facilitating NLTE radiative transfer simulations with very complex atomic models. This NLTE code is based on recently-developed iterative methods for radiative transfer applications (see [31] and references therein). We assume complete frequency redistribution for all the iron lines. We used the so-called 1.5D approximation, *i.e.*, we neglected the effects of *horizontal radiative transfer* on the atomic level populations. As discussed by Shchukina & Trujillo Bueno [31] this is expected to be a good approximation for determining the stellar iron abundance from Fe I and Fe II lines. Kiselman & Nordlund [22] already demonstrated that it is also a good approximation for the oxygen IR triplet.

We have chosen 33 Fe I and 15 Fe II lines for our 3D and 1D determinations of the iron abundance in the halo subgiant HD 140283. The equivalent widths (W) were obtained from high-resolution spectra observed a few years ago with the Harlan J. Smith 2.7-m telescope at the McDonald Observatory (R. García López, private communication; see also [2]). Our Fe II line list includes five weak lines contained in Table 3 of the paper of Nissen *et al.* [27].

The O I IR triplet lines in the metal-poor star HD 140283 are weak. Given uncertainties in the measurements, we have averaged their equivalent widths over three sets of published observations. The resulting equivalent widths of the 7771.96, 7774.18, and 7775.40 Å lines used in our oxygen abundance determinations are 7.9, 4.8, 3.4 mÅ, respectively. The equivalent width of the forbidden [O I] λ 6300 Å line ($W = 0.5$ mÅ) has been taken from the paper [27].

Measurements of the equivalent widths in the solar O I IR lines tend to have an uncertainty of ~5%. Therefore, we have used averaged values of five published observations at the solar disc centre. The resulting averaged solar equivalent widths for the 7771.96, 7774.18, and 7775.40 Å lines are 81.6, 70.4, 57.2 mÅ, respectively.

Our model atom for Fe is realistic (see [31]). It has 225 Fe I levels and 23 Fe II levels including their multiplet fine structure. The Fe I levels are interconnected by 330 bound-bound radiative transitions, while we have 25 radiative transitions among the Fe II levels. The Fe I diagram is, in fact, complete up to EP = 5.72 eV. At higher energies it contains about 50% of the terms identified now.

Our O I Grotrian diagram is based on the data of Carlsson & Judge [12]. It is also similar to that used by [29]. The diagram has 23 O I fine structure levels and one O II level.

RESULTS AND CONCLUSIONS

The most important conclusions that may be drawn from our analysis for the Fe I and Fe II are the following:

- The Fe I lines in the 3D model of HD 140283 are much weaker in NLTE than in LTE because the UV overionization mechanism produces a strong underpopulation of the Fe I levels in the granular regions. As a result, the NLTE effects on the derived iron abundance are very important, amounting to ~0.9 dex and ~0.6 dex in the 3D and 1D cases, respectively (Fig. 1).

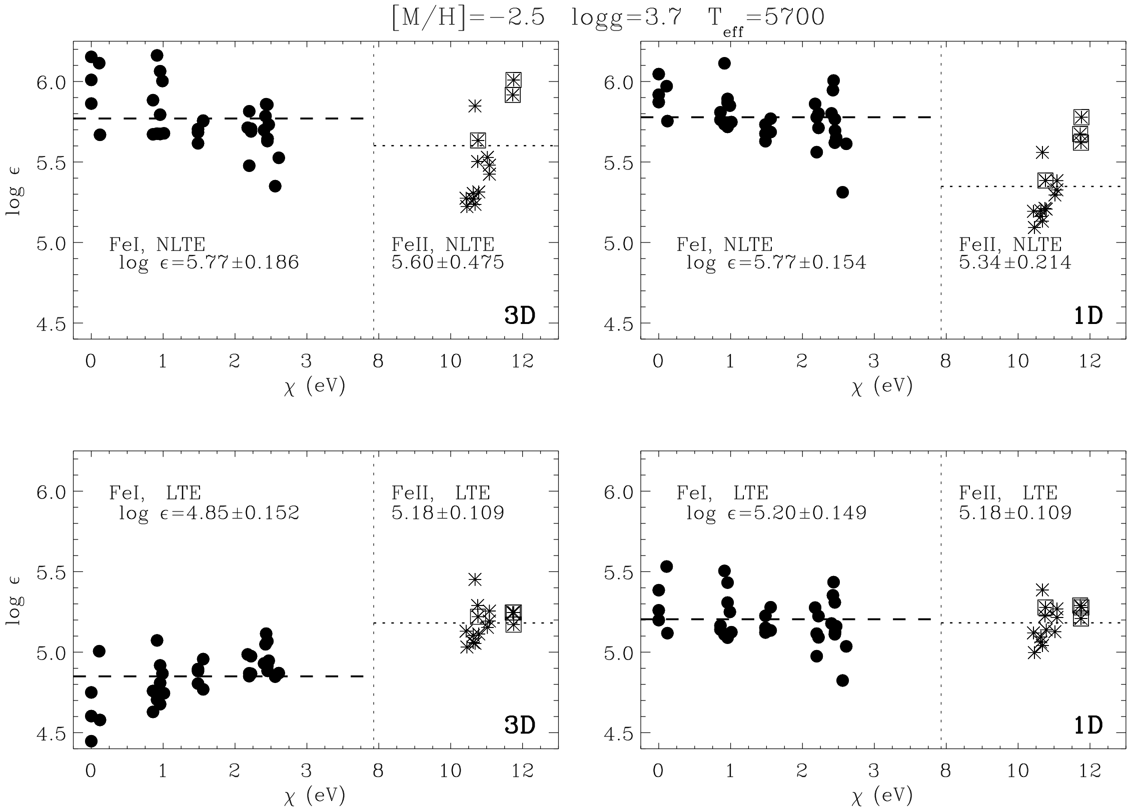

Figure 1. The iron abundances derived from Fe I lines (filled circles) and from Fe I lines (stars) *vs.* the lower level excitation potential χ of the chosen lines. Left panels show the results for the 3D model while the right panels for the 1D model. Top panels: NLTE. Bottom panels: LTE. The four weak Fe II lines ($\lambda\lambda$ 6149.2, 6247.5, 6432.6, 6456.3 Å) used by Nissen *et al.* [27] are marked with squares. The dashed and dotted horizontal lines indicate the mean abundances found from the set of Fe I and Fe II lines, respectively. The mean abundances are given in panels. The stellar parameters used: $T_{\rm eff} = 5700$ K, [Fe/H] $= -2.5$, $\log g = 3.7$

- Under NLTE the Fe I spectrum of the metal-poor subgiant HD 140283 is insensitive to the 3D effects (Fig. 1).
- The NLTE and 3D effects have to be taken into account for a reliable determination of the iron abundances in the HD 140283 from weak Fe II lines because the significant overexcitation of their upper levels in the granules tend to produce emission features (Fig. 2). Such Fe II lines are weaker than in LTE: the abundance correction is $\sim$0.4 dex for the 3D case.
- The solar iron abundance appears to be fairly well determined now ($\log \epsilon_\odot$(Fe) $= 7.50 \pm 0.03$; see our earlier study [31]) – that is, it is similar to the meteoritic value.

Concerning the oxygen abundance determinations it is important to point out the following:

- We derived the oxygen abundance in the HD 140283 by using the O I triplet at λ 7772–5 Å and the forbidden [O I] line at λ 6300 Å. While the oxygen abundance derived from O I triplet is, in fact, insensitive to the presence of granulation inhomogeneities, such 3D effects amount to ~ -0.2 dex for the [O I] line. The NLTE abundance correction for the O I triplet is ~ -0.2 dex.
- We derived the solar oxygen abundance by fitting the observed disc centre profiles (Fig. 3) and equivalent widths of the O I triplet via synthesis in the 3D model. Taking into account NLTE effects we find $\log \epsilon_\odot(\mathrm{O}) = 8.70 \pm 0.06$ while the LTE approximation gives $\log \epsilon_\odot(\mathrm{O}) = 8.93 \pm 0.06$.

There are several discrepancies indicating that the iron abundance results for the star HD 140283 shown in Fig. 1 cannot be considered as reliable, neither in the 1D case nor in the 3D case. For example, we have (1) a divergence of the average abundances derived from both ionization stages, (2) a correlation of the abundances derived from Fe I lines with the lower-level excitation potential and (3) a large scatter in the abundances derived

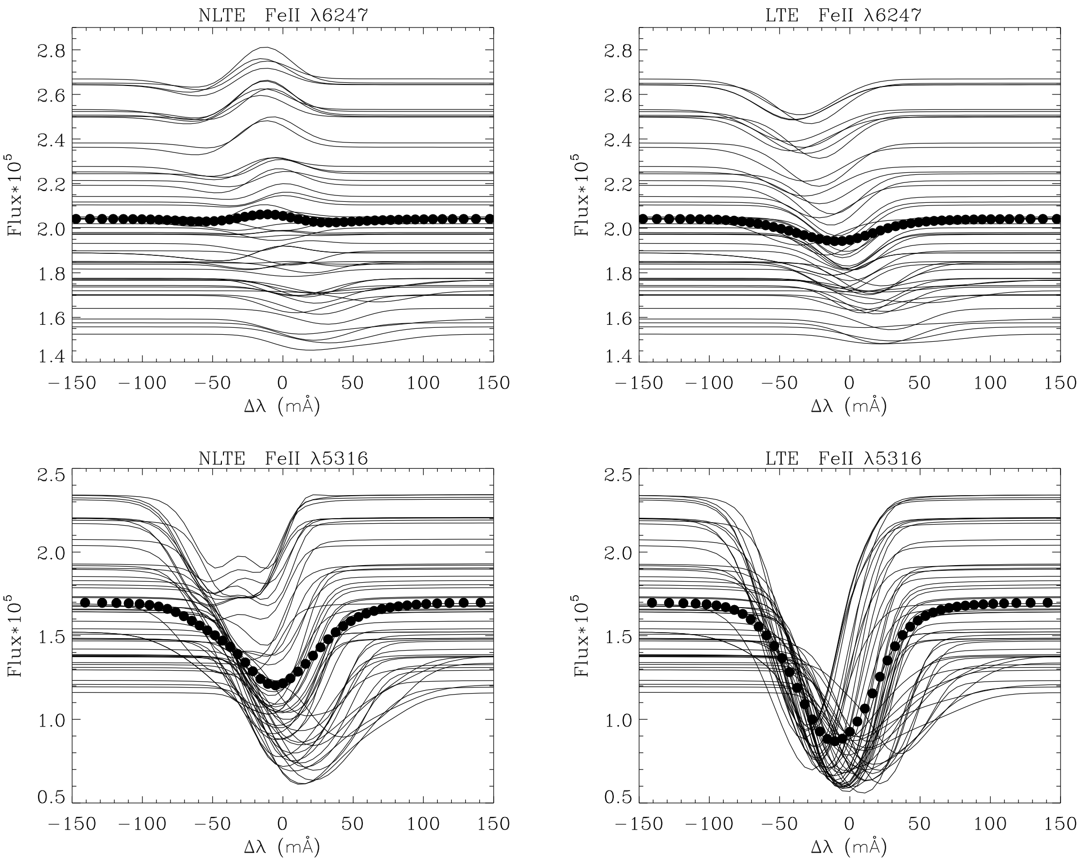

Figure 2. The flux profiles of the weak Fe II $\lambda\,6247.56$ Å line (top panels) and of moderately strong Fe II $\lambda\,5316.62$ Å line (bottom panels) calculated in the 3D hydrodynamical model of the metal-poor subgiant HD 140283. The profiles were synthesized using the iron abundance $\log\epsilon = 5.0$. Left panels: NLTE. Right panels: LTE. Individual thin curves show the computed emergent fluxes for the "granular" and "intergranular" models corresponding to the 50 spatial gridpoints located along one of the slices $Y = 24$. The thick solid lines with filled circles on each of the panels: the resulting spatially averaged flux. The intergranular profiles have a redshift and a lower continuum flux. Bright granules are characterized by a higher continuum flux and a blue line shift. Note that the flux profile of the weak Fe II $\lambda\,6247.56$ Å line is observed in absorption while the synthesized NLTE flux profile is in emission. Fluxes are given in absolute energy units (erg cm^{-2} s^{-1} Hz^{-1})

from Fe II lines (particularly, the weak ones). Our study shows that the elimination of any of such discrepancies cannot be simply achieved in terms of uncertainties in observed equivalent widths, oscillator strengths, collisional rates, photoionization cross sections, continuum opacity, *etc.* The only way we have found for reducing such discrepancies is to revise the stellar parameters of the subgiant HD 140283. Our analysis for the revision of the stellar parameter is based on the following criteria:

i) the average abundances obtained from Fe I and Fe II lines have to be equal.

ii) the "best choice" solution has to give the minimum mean standard deviation (σ) for the abundances derived from Fe I and Fe II lines.

iii) abundances have to be independent of the lower excitation potential (χ).

We restrict ourselves to revise only the metallicity and the effective temperature. The given surface gravity of the star HD 140283 is reliable, since it has been obtained from accurate *Hipparcos* parallaxes. We conclude the following:

- The effective temperature has to be decreased from $T_{\rm eff} = 5700$ K to $T_{\rm eff} = 5600$ K while the metallicity has to be increased from [Fe/H] $= -2.5$ to [Fe/H] $= -2.0$.
- The [O/Fe] ratio equals $+0.5$ at the stellar metallicity [Fe/H] $= -2$.

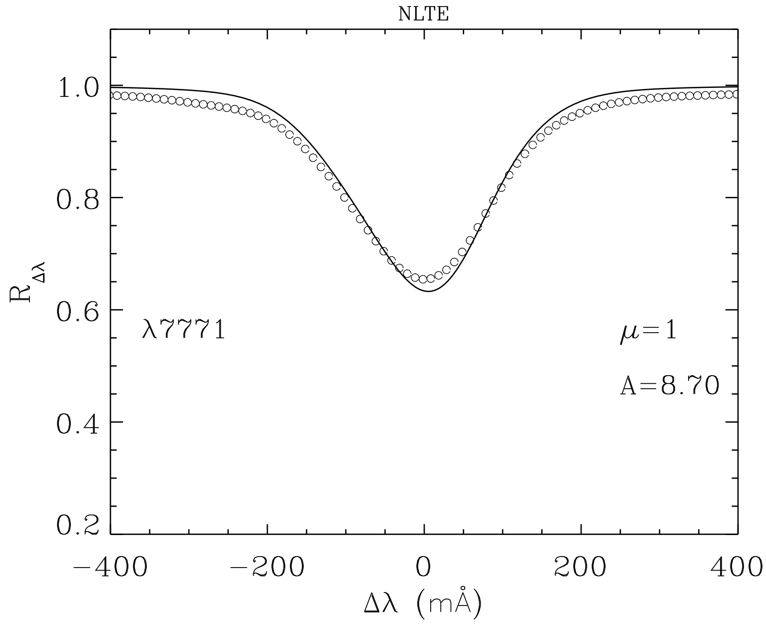

Figure 3. The spatially averaged intensity profile of the strongest line $\lambda\,7771.96$ Å of the O I IR triplet 7772–5 Å for the solar disc centre. Solid line: NLTE calculations in the 3D hydrodynamical model of the Sun. Filled circles: observations (Jungfraujoch atlas [16]). The solar oxygen abundance is $\log \epsilon_{\odot}(\mathrm{O}) = 8.70$

At first sight, such a value falls on the linear rise trend in the [O/Fe]−[Fe/H] diagram. On the other hand, such a value supports the possibility of a plateau between 0.4 and 0.5 dex in the range $-3 <$ [Fe/H] < -1. The analysis of a single metal-poor star is not enough to opt for one of these two possibilities.

Acknowledgements. We are grateful to Ramon García López and Garik Israelian for allowing us to use their stellar observations, and Martin Asplund for 3D models. This work has been funded by the European Commission through INTAS grant 00-00084 and by the Spanish Ministerio de Ciencia y Tecnologia through project AYA2001-1649.

[1] *Abia C., Rebolo R.* Oxygen abundances in unevolved metal-poor stars – Interpretation and consequences // Astrophys. J.–1989.–**347**.–P. 186–194.

[2] *Allende Prieto C., García López R. J., Lambert D. L., Gustaffson B.* Spectroscopic observations of convective patterns in the atmospheres of metal-poor stars // Astrophys. J.–1999.–**526**.–P. 991–1000.

[3] *Allende Prieto C., Lambert D. L., Asplund M.* The forbidden abundance of oxygen in the Sun // Astrophys. J.–2001.–**556**.–P. L63–L66.

[4] *Asplund M.* Stellar abundance analyses in the light of 3D hydrodynamical model atmospheres // Modelling of Stellar Atmospheres: Proc. IAU Symp. 210 / Eds N. Piskunov, W. W. Weiss, D. F. Gray.–Astron. Soc. Pacif., 2003.–P. 273.

[5] *Asplund M., García Pérez A. E.* On OH line formation and oxygen abundances in metal-poor stars // Astron. and Astrophys.–2001.–**372**.–P. 601–615.

[6] *Asplund M., Grevesse N., Sauval A. J., et al.* Line formation in solar granulation. IV // Astron. and Astrophys.–2004.–**417**.–P. 751–768.

[7] *Asplund M., Ludwig H.-G., Nordlund Å., Stein R. F.* The effects of numerical resolution on hydrodynamical surface convection simulations and spectral line formation // Astron. and Astrophys.–2000.–**359**.–P. 669–681.

[8] *Asplund M., Nordlund Å., Trampedach R., Stein R. F.* 3D hydrodynamical model atmospheres of metal poor stars. Evidence for a low primordial Li abundance // Astron. and Astrophys.–1999.–**346**.–P. L17–L20.

[9] *Athay R. G., Lites B. W.* Fe I ionization and excitation equilibrium in the solar atmosphere // Astrophys. J.–1972.–**176**.–P. 809–831.

[10] *Barbuy B.* Oxygen in 20 halo giants // Astron. and Astrophys.–1988.–**191**.–P. 121–127.

[11] *Boesgaard A. M., King J. R., Deliyannis C. P., Vogt S.* Oxygen in unevolved metal-poor stars from Keck ultraviolet HIRES spectra // Astron. J.–1999.–**117**.–P. 492–507.

[12] *Carlsson M., Judge P.* O I lines in the Sun and stars. I – Understanding the resonance lines // Astrophys. J.–1993.–**402**.–P. 344–357.

[13] *Carretta E., Gratton R. G., Sneden C.* Abundances of light elements in metal-poor stars. III. Data analysis and results // Astron. and Astrophys.–2000.–**356**.–P. 238–252.

[14] *Cavallo R. M., Pilachowski C. A., Rebolo R.* Oxygen Abundances in metal poor subgiant stars from the O I triplet // Astron. Soc. Pacif. Conf. Ser.–1997.–**109**.–P. 226–235.

[15] *Cram L. E., Rutten R. J., Lites B. W.* On the formation of Fe II in stellar spectra. I // Astrophys. J.–1980.–**241**.–P. 374–384.

[16] *Delbouille L., Neven L., Roland G.* Photometric Atlas of the Solar Spectrum from $\lambda\,3000$ to $\lambda\,10{,}000$.–Liegè: Institut d'Astrophysique de l'Université de Liegè, 1973.

[17] *Fulbright J., Kraft R.* Oxygen abundances in two metal-poor subgiants from the analyses of the 6300 Å forbidden O I line // Astron. J.–1999.–**118**.–P. 527–538.

[18] *Israelian G., García López R. J., Rebolo R.* Oxygen abundances in unevolved metal-poor stars from near-ultraviolet OH lines // Astrophys. J.–1998.–**507**.–P. 805–817.

[19] *Israelian G., Rebolo R., García López R. J., et al.* Oxygen in the very early Galaxy // Astrophys. J.–2001.–**551**.–P. 833–851.

[20] *Israelian G., Shchukina N., Rebolo R., et al.* Oxygen and magnesium abundance in the ultra-metal-poor giants CS 22949-037 and CS 29498-043: Challenges in models of atmospheres // Astron. and Astrophys.–2004.–**419**.–P. 1095–1109.

[21] *Kiselman D.* NLTE effects on oxygen lines // New Astron. Rev.–2001.–**45**, Issue 8.– P. 559–563.

[22] *Kiselman D., Nordlund Å.* 3D non-LTE line formation in the solar photosphere and the solar oxygen abundance // Astron. and Astrophys.–1995.–**302**.–P. 578.

[23] *Kostik R. I., Shchukina N. G., Rutten R. J.* The solar iron abundance: not the last word // Astron. and Astrophys.–1996.–**305**– P. 325–342.

[24] *Kraft R. P., Sneden C., Langer G. E., Prosser C. F.* Oxygen abundances in halo giants. II. Giants in the globular clusters M13 and M3 and the intermediately metal-poor halo field // Astron. J.–1992.–**104**.–P. 645–668.

[25] *Meléndez J., Barbuy B.* Keck NIRSPEC infrared OH lines: oxygen abundances in metal-poor stars down to [Fe/H] $= -2.9$ // Astrophys. J.–2002.–**575**.–P. 474–483.

[26] *Mishenina T., Korotin S., Klochkova V., Panchuk V.* Oxygen abundance in halo stars from O I triplet // Astron. and Astrophys.–2000.–**353**.–P. 978–986.

[27] *Nissen P. E., Primas F., Asplund M., Lambert D. L.* O/Fe in metal-poor main sequence and subgiant stars // Astron. and Astrophys.–2002.–**390**.–P. 235–251.

[28] *Rutten R. J.* The NLTE formation of iron lines in the solar spectrum // Physics of formation of Fe II lines outside LTE: IAU Colloq. 94 / Eds R. Viotti, A. Vittone, M. Friedjung.–Dordrecht: Reidel, 1988.–P. 185–210.

[29] *Shchukina N. G.* The effects of departure from the local thermodynamical equilibrium in the solar Fraunhofer spectrum. Oxygen // Kinematics and Physics of Celestial Bodies.–1987.–**3**, N 6.–P. 33–42.

[30] *Shchukina N. G., Vasiljeva I. E., Trujillo Bueno J., Asplund M.* Stellar granulation and the NLTE formation of the Fe I and O I lines: the metal-poor star HD 140283 // Modelling of Stellar Atmospheres: Proc. IAU Symp. 210 / Eds N. Piskunov, W. W. Weiss, D. F. Gray.–Astron. Soc. Pacif., 2003.–B10.

[31] *Shchukina N., Trujillo Bueno J.* The iron line formation problem in three-dimensional hydrodynamical models of solar-like photospheres // Astrophys. J.–2001.–**550**.–P. 970–990.

[32] *Shchukina N. G., Trujillo Bueno J.* The impact of non-LTE effects and granulation inhomogeneities on the derived iron and oxygen abundances in metal-poor halo stars // Astrophys. J.–2004.

[33] *Stein R. F., Nordlund Å.* Simulations of solar granulation. I. General properties // Astrophys. J.–1998.–**499**.–P. 914–933.

[34] *Takeda Y.* Oxygen line formation in late-F through early-K disk/halo stars. Infrared O I triplet and [O I] lines // Astron. and Astrophys.–2003.–**402**.–P. 343–359.

[35] *Thévenin F., Idiart T.* Stellar iron abundances: non-LTE effects // Astrophys. J.–1999.–**521**.–P. 753–763.

[36] *Tomkin J., Lemke M., Lambert D. L., Sneden C.* The carbon-to-oxygen ratio in halo dwarfs // Astron. J.–1992.–**104**.–P. 1568–1584.